Synthetic Metals 161 (2011) 2017–2023

Contents lists available at ScienceDirect

Synthetic Metals

journal homepage: www.elsevier.com/locate/synmet

High performance battery–supercapacitor hybrid energy storage system based on self-doped polyaniline nanofibers

H.R. Ghenaatian [a], M.F. Mousavi [a,*], M.S. Rahmanifar [b]

[a] Department of Chemistry, Tarbiat Modares University, P.O. Box 14115-175, Tehran, Iran
[b] Faculty of Basic Science, Shahed University, Tehran, Iran

ARTICLE INFO

Article history:
Received 21 December 2010
Received in revised form 10 June 2011
Accepted 20 July 2011
Available online 15 August 2011

Keywords:
Hybrid power source
Supercapacitor
Secondary battery
Self-doped polyaniline nanofiber

ABSTRACT

Nanostructured self-doped polyaniline (SDPA) is prepared from an aqueous solution of aniline and *m*-aminobenzoic acid using an electrochemical method onto a stainless steel electrode. This electrode employed as a positive shared electrode in the construction of a hybrid battery–supercapacitor energy storage system AC/SDPA/Zn. This hybrid system is constructed using a parallel combination of an asymmetric supercapacitor (AC/SDPA) and a secondary battery (Zn/SDPA) in a single cell configuration and same electrolyte. Different electrochemical methods including cyclic voltammetry, galvanostatic charge–discharge and rate charge–discharge studies are carried out to characterize electrochemical performances of the hybrid system. Based on the obtained results, the hybrid system shows specific capacity, specific energy, specific power and maximum power values of 215 Ah kg^{-1}, 204 Wh kg^{-1}, 863 W kg^{-1} and 8909 W kg^{-1}, respectively, at a current density of 2.5 mA cm^{-2}.

1. Introduction

Nanoscale materials have opened a new rich world of possibilities for science and engineering and widely used in many fields [1,2]. The electroactive nanomaterials can improve the performance of electrochemical energy storage systems such as batteries and supercapacitors [3]. It is due to more efficient electrochemical reactions of nanomaterials in these two energy storage systems as compared to micromaterials [4,5]. So, using electroactive nanomaterials, the performance of such systems is extremely improved and specific capacity of batteries and supercapacitors get close to the theoretical values.

The ability to store transiently and redeliver high energy and high power electric energy in the modern energy storage systems is an essential component of today's hybrid electric devices. In such electric systems, performance requirements are high energy density, high rate charge acceptance-delivery and long cycle life [6–9]. Supercapacitors and secondary batteries are energy storage systems; however, in practical applications, none of them can be properly used as a single power supply for hybrid electric devices due to low energy and low power characteristics of supercapacitors and secondary batteries, respectively [10–13]. A parallel combination of these two energy storage systems provides a high power hybrid energy storage system which simultaneously shows high energy and high power characteristics of batteries and supercapacitors, respectively [14,15]. They could be used in parallel (separated cells) and/or shared electroactive materials and electrolytes (single unit cell). However, it does not mean that the hybrid energy storage systems can be easily achieved by combining any supercapacitor with any secondary battery because of their difference in the operational voltage range [16]. If the operational voltage range of supercapacitor is not equal to the secondary battery, one of them is always at the overcharge state and undergoes irreversible reactions and the other is always at the discharge state. So the hybrid energy storage system works with poor performance. Moreover, the simple parallel design of any supercapacitor with any secondary battery with the same working voltage cannot reach hybrid power source; it is due to the difference in charging/discharging slope of these two systems. So, it is necessary to use a DC–DC converter because charging or discharging of the supercapacitor is done up or down to the secondary battery voltage level. The single cell configuration of hybrid energy storage systems is more interesting than separated cell configuration because in these systems, the DC–DC converter does not need and has a higher specific gravimetric/volumetric energy and power due to use of shared electroactive material and the same electrolyte [17]. With this design, the total charge and discharge currents of the hybrid energy storage systems are composed of both supercapacitor and secondary battery current.

Among the wide variety of electrically conducting polymers (ECPs) polyaniline (PAN) nanostructures as an advanced materials

* Corresponding author. Tel.: +98 21 82883474/82883479; fax: +98 21 88006544.
E-mail addresses: mfmousavi@yahoo.com, mousavim@modares.ac.ir (M.F. Mousavi).

0379-6779/$ – see front matter © 2011 Elsevier B.V. All rights reserved.
doi:10.1016/j.synthmet.2011.07.018

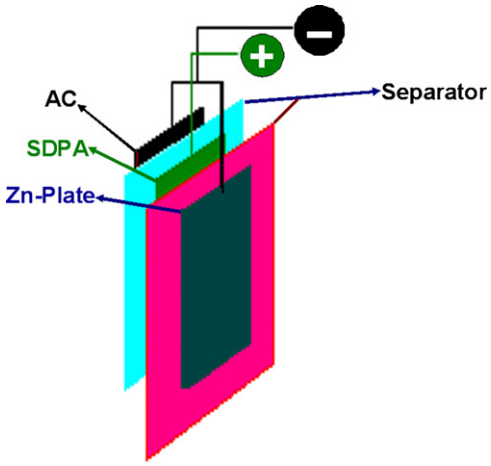

Fig. 1. Schematic view of AC/SDPA/Zn hybrid cell: SDPA as positive shared electrode, electrodeposited on a stainless steel current collector, cellulose acetate separator and activated carbon (AC), pressed on a stainless steel current collector, and Zn plates as negative electrodes.

with high surface area and high porosity give the best performances in the PAN–Zn secondary batteries with aqueous electrolytes [18]. A difficulty arises when Zinc is the counter electrode, since Zinc undergoes spontaneous dissolution in acidic media, while PAN is electroactive only in acidic media [19–22]. The other difficulty is PAN degradation in the aqueous medium [23] which causes lowering the OCV of PAN–Zn battery [24]. Studies show that some steric reagents reduce the rate of PAN degradation [25]. Unlike PAN, its derivatives, e.g. SDPA exhibit better chemical stability due to steric protection by the carboxylic and sulfonic group [26]. In addition, the SDPA does not lose its electrochemical activity in low acidic solutions. Because in the charge–discharge cycles of energy storage systems, the reversible exchanging of anions among ECP and electrolyte limits very important characteristics such as available power that slakes due to limited rate of anions mobility [27–29]. However, SDPA excludes the participation of functional groups with negative charge (like $-COO^-$ and $-SO^{3-}$), which eliminates the ion mobility problem. So, by employing SDPA, the carboxylic group of the *m*-aminobenzoic acid can locally provide both necessary proton and anionic dopants in the polymer's network. So, polymer electroactivity does not need the external protons in the solution. In other words, SDPA enables one to work in mild pH which provides the following advantages: (i) retain the polymer electroactivity, (ii) decrease polymer degradation and (iii) decrease spontaneous Zn dissolution. So, SDPAs are expected to be promising electroactive materials for the positive electrodes in Zinc and Lithium secondary batteries [30–33].

In previous reports, we constructed a secondary battery [21] and a symmetric supercapacitor [34] using SDPA and Platinum as electroactive material and current collector, respectively. Although this system shows a high specific capacitance 480 F g^{-1}, the limited application of the symmetric supercapacitor SDPA/SDPA due to its low working voltage does not let it parallel with the secondary battery Zn/SDPA. It should be noted that the symmetric supercapacitors are constructed with two similar electroactive materials which reach maximum 1.2 V in the aqueous electrolyte solutions. Whereas, the asymmetric supercapacitors are assembled using a positive electrode with the large positive cutoff potential and a negative electrode with high hydrogen overpotential, which results in a significant increase in the overall cell operating voltage in the aqueous solutions. Therefore, by employing asymmetric supercapacitor configuration, one can extend the operational cell voltage as reported by Park and Park [35] as 1.6 V and by Wang et al. [36] as 1.4 V for asymmetric supercapacitor AC/PAN.

Following our recent works on improving the performance of lead acid [37,38], dry and wet Zn–PAN batteries [39–42], and more recent studies on using SDPA nanofibers as a new material for symmetric redox supercapacitor [34]. Herein, we introduce a new high power–energy hybrid power source using a parallel combination of high operational voltage aqueous asymmetric supercapacitor with a secondary battery in a mild pH. In this system, to improve the performance, the working voltage of the symmetric supercapacitor SDPA/SDPA was increased by replacing of SDPA negative electrode with activated carbon (AC). So, the operational working voltage of this asymmetric configuration (AC/SDPA) was tuned to match with the secondary battery Zn/SDPA. This is an essential requirement for construction of a hybrid battery–supercapacitor. Different electrochemical methods including cyclic voltammetry, galvanostatic charge–discharge and rate charge–discharge studies are carried out to characterize electrochemical performances of the AC/SDPA/Zn hybrid energy storage system.

2. Experimental

2.1. Chemicals

AC, reagent grade *m*-aminobenzoic acid and aniline were obtained from Merck and Fluka. Aniline was doubly distilled and kept under argon in darkness at 5 °C. HCl, NH_4Cl and $ZnCl_2$ were prepared from Merck as analytical grade chemicals. Doubly distilled water was used to prepare all solutions.

2.2. Methods

An Autolab PGSTAT 30 instrument (Eco-Chemie, The Netherlands) was used for electrochemical depositions and measurements. Electrodeposition of SDPA was carried out in a conventional three electrode cell. The stainless steel (SS, grade 304, 0.5 mm thickness) plate (2 cm × 2 cm) was used as the working electrode, a Pt plate and Ag/AgCl (KCl, saturated) were utilized as counter and reference electrodes, respectively.

Electrochemical studies on the hybrid system were performed using a lab-made three electrode configuration cell that is shown in Fig. 1. In this cell, a shared SDPA acts as the positive pole of Zn-secondary battery and asymmetric supercapacitor. Zn plate and AC were used as negative poles in the Zn-secondary battery and asymmetric supercapacitor. Positive plate was separated from negative plates using cellulose acetate as a separator. The AC was coated on SS plate (2 cm × 2 cm) by mixing 90 wt% of AC powder with 10 wt% of poly(tetraflouroethylene) (PTFE). This resulted in a rubber-like paste that was rolled in a film (about 2 mm thick) on a flat SS surface and dried 12 h at 60 °C. Then to assure a good electrical contact, electrode was hot-pressed under a pressure of 15 MPa at 110 °C for 3 min. Before the electrochemical measurements, the AC electrode must be activated by immersing it into 1.0 M $ZnCl_2$ and 0.5 M NH_4Cl mixed electrolyte solution for 24 h. Scanning electron microscopy (SEM) was performed with a Philips instruments, Model X-30. All experiments were carried out at 25 °C in an air-conditioned room.

2.3. Electrodeposition of SDPA

SDPA nanofibers were potentiostaticaly deposited on the SS plate at the potential of 0.85 V vs. Ag/AgCl in an electrolyte solution of 1 M HCl + 0.05 M aniline + 0.05 M *m*-aminobenzoic acid. Before electrodeposition of SDPA, SS electrodes were polished using slurry (particle size 0.5 μm), washed in water and ethanol. Then the modified electrodes were washed with 1.0 M HCl solution to perform

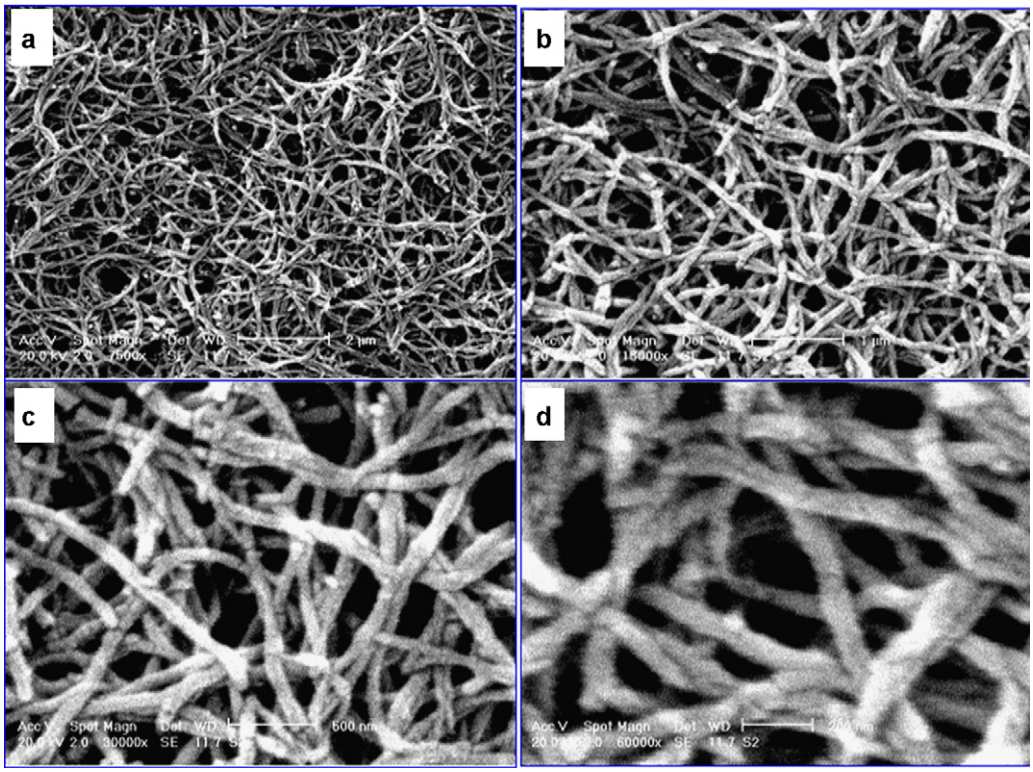

Fig. 2. Scanning electron micrographs of self-doped polyaniline nanofibers in the different magnifications.

electrochemical studies such as galvanostatic charge–discharge, rate charge–discharge and cyclic voltammetry (CV) in 1.0 M $ZnCl_2$ and 0.5 M NH_4Cl mixed electrolyte solution. Also the stability and power–energy characteristics of the battery–supercapacitor hybrid system were studied in detail by charge–discharge experiments. To evaluate the quantity of the active material onto the plates, the SS electrodes were weighed before and after SDPA coating procedure.

3. Results and discussion

3.1. SEM analysis of SDPA nanofibers

Since the formation of the nanofibers is highly dependent upon the substrate nature and applied potential, it is worthwhile to compare our results with those of other investigations. Gupta and Miura [43] reported that the synthesis of polyaniline nanowires has been achieved potentiostaticaly at the constant potential of 0.75 V vs. SCE (0.79 V vs. Ag/AgCl) on the stainless steel, whereas in the present study, aniline and *m*-aminobenzoic acid monomers have been used to prepare SDPA nanofibers. It is noteworthy that the presence of carboxylic group in *m*-aminobenzoic acid deactivates its aromatic system with respect to an electrophilic substitution due to the electron-withdrawing effect. Therefore, this electronic effect is also responsible for the higher potential (0.85 V vs. Ag/AgCl) needed to oxidize the *m*-aminobenzoic acid monomers, compared to aniline.

SDPA nanofiber formation mechanism is a typical bottom-up approach in which aniline and *m*-aminobenzoic acid (monomers) primarily produce corresponding cation radicals, followed by attaching to other monomers to produce oligomers. A further progress results in extended length in intertwined nanofibers and cross-links lead to 3-dimensional network of SDPA [43]. It should be mentioned that by increasing the oligomers length, Ohmic drop increases and leads to the formation of the cation radicals at higher potentials. However, SDPA has autocatalysis effect that leads to decreasing radical-cation formation. These two compensation effects cause the formation of uniform nanofibers in thin layers of polymer. Therefore, the classical theory of nucleation and growth can be used to describe the mechanism of nanofiber film formation [44–47].

Fig. 2a–d shows the SEMs of SDPA thin films in different magnifications (7500, 15,000, 30,000 and 60,000×). As it is seen, the SDPA film consisted of uniform nanofibers with diameters in the range of 70–90 nm.

3.2. Cyclic voltammetry studies

Fig. 3a–c shows cyclic voltammograms of supercapacitor AC/SDPA and secondary battery Zn/SDPA in the two-electrode system and AC/SDPA/Zn in the hybrid cell (Fig. 1) at scan rate of 5 mV s^{-1} into 1.0 M $ZnCl_2$ and 0.5 M NH_4Cl mixed electrolyte solution, respectively. As it shown in Fig. 3a, supercapacitor AC/SDPA represents a parallelogram box-like shape between 0.4 and 1.5 V and exhibits high quality supercapacitive behavior with excellent reversibility (the CV of an ideal supercapacitor without internal resistance would have a rectangular shape. When taking into account internal resistance, the CV gets a shape close to parallelogram with two smoothed over angles). This asymmetric supercapacitor includes both a polarizable (AC) and a non-polarizable (SDPA) electrode. As it is shown schematically as following, charge storage mechanisms in the AC/SDPA are non-Faradaic and Faradaic.

$$\text{Positive}: \quad \mathrm{SDPA_{red}} \underset{\text{discharge}}{\overset{\text{charge}}{\rightleftarrows}} \mathrm{SDPA_{ox}} + \mathrm{ne} \tag{1}$$

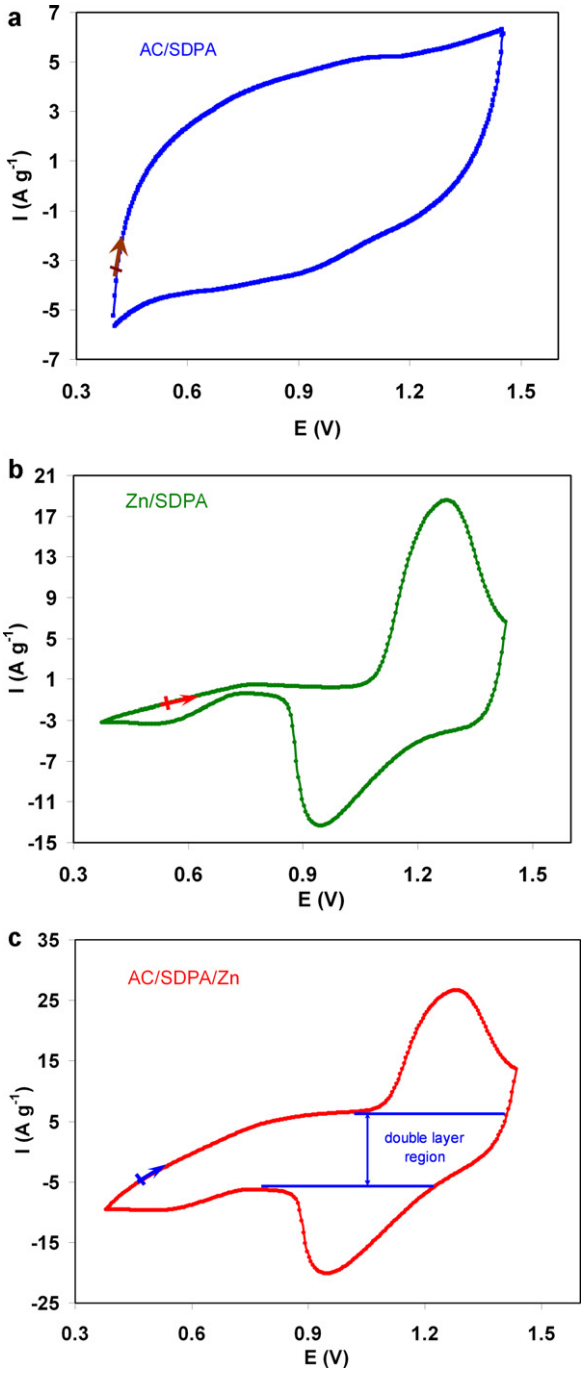

Fig. 3. CV curves of the (a) AC/SDPA supercapacitor, (b) Zn/SDPA secondary battery and (c) battery–supercapacitor hybrid system AC/SDPA/Zn in 1.0 M $ZnCl_2$ and 0.5 M NH_4Cl mixed electrolyte solution at scan rate of 5 mV s^{-1}.

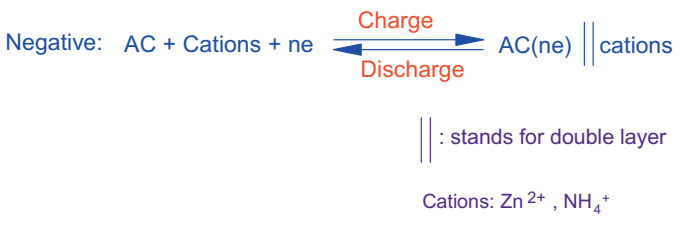

(2)

When the supercapacitor is charged in a Faradaic process, $SDPA_{red}$ is converted to $SDPA_{ox}$ and electrons flow to negative electrode. Then, according to charge neutrality, positive ions are absorbed onto the carbon negative electrode – non-Faradaic process – to balance its charges.

In order to evaluate tunability of the secondary battery Zn/SDPA with supercapacitor AC/SDPA for constructing hybrid AC/SDPA/Zn using a shared SDPA positive electrode, cyclic voltammogram of the Zn/SDPA system was recorded (Fig. 3b). As it is shown, this system similar to the supercapacitor AC/SDPA (Fig. 3a) can be charge/discharged in the sloping form in the voltage range between 0.4 and 1.5 V.

Fig. 3c shows the cyclic voltammogram of the hybrid AC/SDPA/Zn in the similar voltage range (0.4–1.5 V). As seen in Fig. 3b and c, the secondary battery SDPA/Zn and the hybrid AC/SDPA/Zn exhibit two current peaks. The peaks at 1.29 V and 0.98 V are related to, respectively, charge and discharge behavior of these two energy storage systems which can be shown schematically as following:

$$SDPA_{red} + Zn^{2+} \underset{\text{discharge}}{\overset{\text{charge}}{\rightleftarrows}} SDPA_{ox} + Zn \quad (3)$$

However, as it is shown in Fig. 3c, unlike the secondary battery SDPA/Zn which stores energy only in Faradaic mechanism, hybrid AC/SDPA/Zn represents a bigger response current (curve in a rectangle) that is related to non-Faradaic (electrically double layers (EDLs)) storage energy more than Faradaic mechanism which is related to adjoin AC component. Moreover, these two systems exhibit different electrochemical behaviors in the lower potential range. As Fig. 3b and c shows, the hybrid AC/SDPA/Zn exhibits higher capacitive current than the SDPA/Zn battery. The above results from CVs demonstrate that by the addition of AC in the hybrid AC/SDPA/Zn, the rate of the electron transfer does not change because peak separation is approximately equal to the SDPA/Zn battery, but, energy storage in the hybrid AC/SDPA/Zn is done in the wider potential range using a double layer in addition to Faradaic energy storage. However, the hybrid AC/SDPA/Zn system shows that the performance extends into higher ability for energy storage inaccessible to the single system.

3.3. Charge–discharge characteristics

The galvanostatic discharges of the systems are performed at constant discharge current density of 2.5–20 mA cm^{-2} into 1.0 M $ZnCl_2$ and 0.5 M NH_4Cl mixed electrolyte solution and plotted in Fig. 4a–c. As it is shown, the potential dropped sharply at the beginning of each experiment, proportional to the internal resistance (ESR) which includes the electrode and electrolyte solution resistance. It could be calculated according to $R\ (\Omega) = (E_{charge} - E_{discharge})/2I$, where I, E_{charge} and $E_{discharge}$ are the applied constant discharge current (A), the cell voltage at the end of charge and at the beginning of discharge (V), respectively [48,49]. This gives average values of 1.5, 5 and 2 Ω for the supercapacitor AC/SDPA, the secondary battery Zn/SDPA and the hybrid AC/SDPA/Zn, respectively, at constant charge–discharge current density of 2.5 mA cm^{-2}. These values show that the internal resistance of the battery–supercapacitor hybrid system is lower and it has higher power than the battery.

Fig. 4a and b shows galvanostatic discharge profiles of the supercapacitor AC/SDPA and the secondary battery Zn/SDPA, respectively. As it is obvious, these two systems nearly show sloping discharge behavior (Fig. 4a and b) in the voltage windows 0.4–1.5 V. However, unlike the supercapacitor AC/SDPA (Fig. 4a), a secondary battery Zn/SDPA (Fig. 4b) cannot store energy at whole voltage window 0.4–1.5 V which is due to the nature of the negative poles of the

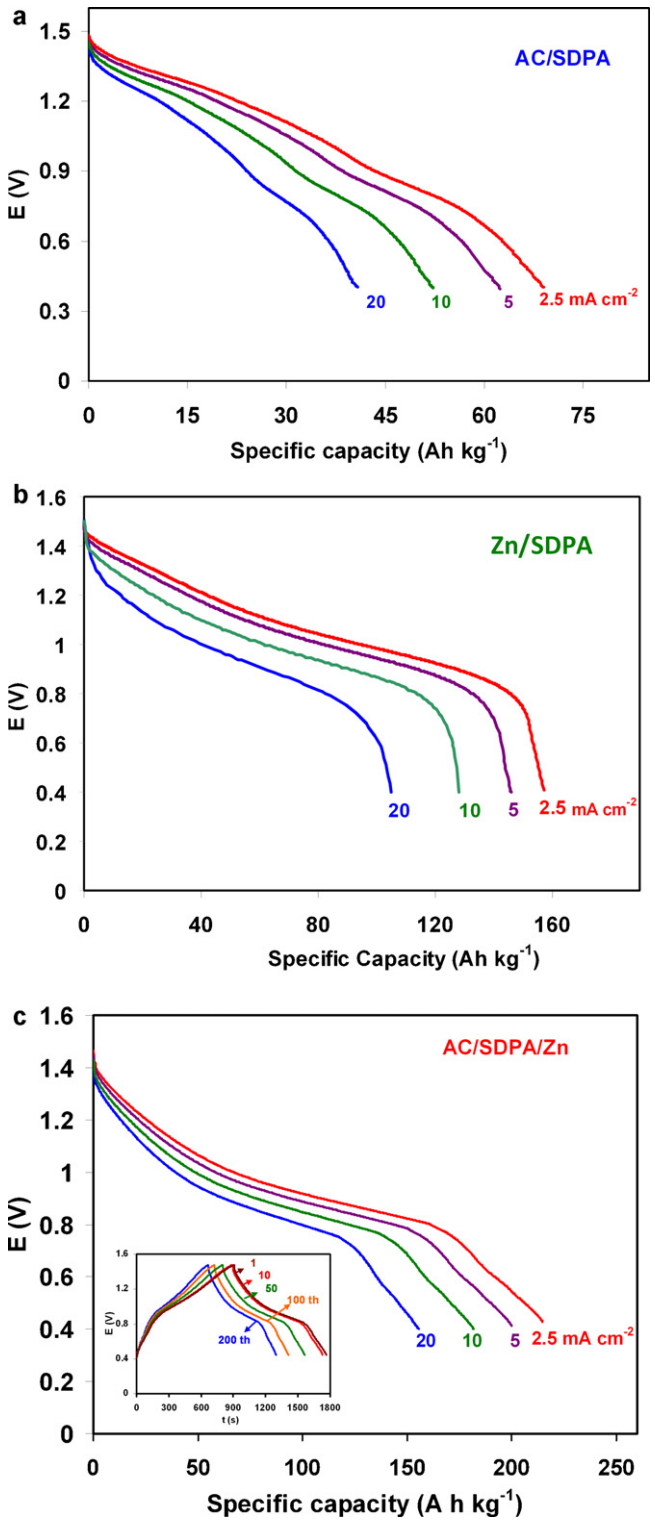

Fig. 4. Galvanostatic charge–discharge curves of (a) AC/SDPA supercapacitor, (b) Zn/SDPA secondary battery and (c) the battery–supercapacitor hybrid system AC/SDPA/Zn at a various constant current density of 2.5–20 mA cm^{-2} into 1.0 M $ZnCl_2$ and 0.5 M NH_4Cl mixed electrolyte solution.

AC/SDPA and the Zn/SDPA systems. However, these two systems can be connected to each other in parallel because their operational voltages are nearly similar and they are tunable. As shown in Fig. 4c, it is obvious that the discharge profile of the hybrid AC/SDPA/Zn exhibits improved electrochemical behavior as compared with the other two and its discharge profile (Fig. 4c) is reconciliation of two

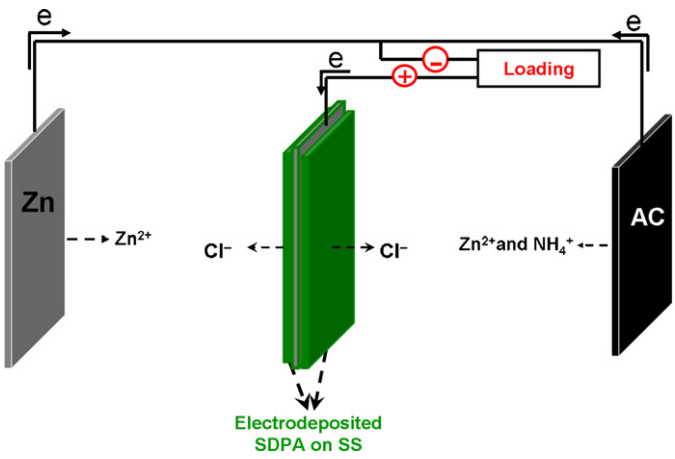

Fig. 5. Schematic representation of the electrochemical/physical exchange takes place between the different materials in the three electrodes of the battery–supercapacitor hybrid system AC/SDPA/Zn at load condition.

other systems. As it is shown, the whole charge/discharge process of the hybrid AC/SDPA/Zn (inset Fig. 4c) does not exhibit obvious sloping voltage profile and has several steps. In the potential ranges of 0.4–1.05 V and 0.8–0.4 V in the charge and discharge processes, respectively, EDLs is dominant charge storage mechanism. However, in the potential range of 1.05–1.5 V and 1.5–0.8 V in the charge and discharge processes, respectively, Faradaic mechanism is dominant. So, comparison of this hybrid AC/SDPA/Zn with a single secondary battery Zn/SDPA showed its discharge performance was superior to that of a single secondary battery Zn/SDPA when the shared SDPA electrode and the same electrolyte medium were adopted.

When the battery–supercapacitor hybrid system is loaded, the electrochemical/physical phenomena take place between different materials (Fig. 5). Electrical energy is produced by the chemical/physical action between the metal and/or AC and the electrolyte. Electrons are transported between the positive and negative electrodes via an external circuit and this process is known as discharging. The material in the Zinc electrode is oxidized and releases electrons to the electrode (Faradaic process), which as a result becomes more negative (an anodic reaction) represented by the following chemical equation.

$$Zn \rightarrow Zn^{2+} + 2e \quad (4)$$

Parallel to the above chemical reaction, some electrons separate from AC (on the charged state AC contain negative charge) and the absorbed cations are desorbed from the AC surface (double layer capacitive process). At the same time, the $SDPA_{ox}$ in the positive electrode is reduced to $SDPA_{red}$ and the electrode becomes less positive (a cathodic electrochemical reaction).

$$SDPA_{ox} + ne \rightarrow SDPA_{red} \quad (5)$$

The electrons flow from Zinc and AC, through external load to the cathode where the electrons are accepted and the cathode material is reduced. The process produces Zn^{2+} and $SDPA_{red}$ on the negative and positive plates, respectively. Also AC was depolarized on discharge time and no chemical reaction occurred on it. The total cell reaction is shown in Fig. 5.

The galvanostatic charge–discharge experiment results for the AC/SDPA, Zn/SDPA and AC/SDPA/Zn cells are shown in Table 1. The specific capacity (SC), specific power (SP), specific energy (SE) and maximum power (P_{max}) accessible for assembled cells were calculated according to the following equations [50]:

$$\text{Specific capacity(SC)} = \frac{It}{3600m}(\text{Ah/kg}) \quad (6)$$

Table 1
Electrochemical performances of various cells.

Cell	I (A g^{-1})	I (A cm^{-2})	$t_{discharge}$ (s)	E_{ave} (V)	Capacity (Ah kg^{-1})	Specific energy (Wh kg^{-1})	ESR (Ω)
Supercapacitor AC/SDPA	3.3	2.5	73	0.95	67 (equal to 230 F g^{-1})	63	1.5
Secondary battery Zn/SDPA	0.83	2.5	678	0.95	157	149	5
Supercapacitor–battery hybrid system AC/SDPA/Zn	0.90	2.5	851	0.95	215	204	2

where t is discharging time (s) and m is the weight of the electrodeposited electroactive materials on the positive pole (SDPA) in the cells.

$$\text{Specific power (SP)} = \frac{E_{ave} I}{m} (\text{W/kg}) \quad (7)$$

where $E_{ave} = (E_{max} + E_{min})/2$ with E_{max} and E_{min} are potential at the end of charge and discharge, respectively.

$$\text{Specific energy (SE)} = \frac{(\text{SP})t}{3600} (\text{Wh/kg}) \quad (8)$$

$$\text{Maximum power (MP)} = \frac{E^2_{discharge}}{4Rm} (\text{W/kg}) \quad (9)$$

where $E_{discharge}$ is the potential at the beginning of discharge (after the Ohmic drop) (V) and R the internal resistance (Ω).

As it is obvious from the CV and charge–discharge results, the application of AC as a supercapacitor component in the AC/SDPA/Zn cell leads to higher specific energy compared to the Zn/SDPA secondary battery with an increase of approximately 31% for equal mass of SDPA (Table 1). The maximum power density is also greatly enhanced with values as high as 8909 W kg^{-1} for the AC/SDPA/Zn cell.

All these results show that the AC/SDPA/Zn hybrid aqueous energy storage system using a secondary battery Zn/SDPA and supercapacitor AC/SDPA exhibits good power–energy characteristics. It is because the high power supercapacitor AC/SDPA and high energy secondary battery Zn/SDPA are tunable.

3.4. Performance of hybrid AC/SDPA/Zn

The Ragon plots for both AC/SDPA/Zn and Zn/SDPA cells derived from results of galvanostatic discharge curves at different current densities are shown in Fig. 6. It is clear from the results that the battery–supercapacitor hybrid system AC/SDPA/Zn exhibit outstanding performances compared with that of the secondary battery Zn/SDPA. For example, at a constant current density of 2.5 mA cm^{-2}, the best specific energy of 204 Wh kg^{-1} was obtained at the corresponding specific power of 863 W kg^{-1} whereas specific energy of 149 Wh kg^{-1} was obtained for Zn/SDPA secondary battery.

The corresponding high-rate dischargeability (HRD) was used to research the power property of the hybrid AC/SDPA/Zn and the secondary battery Zn/SDPA calculated according to Eq. (10), which are also depicted in Fig. 7.

$$\text{HRD (\%)} = \frac{C_d}{C_1} \times 100 \quad (10)$$

where C_d is the discharge capacity of the hybrid AC/SDPA/Zn and the secondary battery Zn/SDPA at a certain current density and C_1 is their discharge capacity at 2.5 mA cm^{-2} [51].

Comparison between the hybrid AC/SDPA/Zn and secondary battery Zn/SDPA in Fig. 7, nicely shows the buffering effect of the supercapacitor AC/SDPA in the hybrid AC/SDPA/Zn especially in high discharge rate (20 mA cm^{-2}). In this current density, HRD (%) for the secondary battery Zn/SDPA is 67% and for the hybrid AC/SDPA/Zn is 79%. This improvement confirms the system has been correctly designed and tuned.

The battery–supercapacitor hybrid system AC/SDPA/Zn was subjected to a prolonged cycle-life test at a constant discharge current density of 2.5 mA cm^{-2} into 1.0 M $ZnCl_2$ and 0.5 M NH_4Cl mixed electrolyte solution for 200 cycles and the resulting specific capacity vs. cycle number plots are shown in Fig. 8. As it is obvious, the hybrid AC/SDPA/Zn exhibits good cycling life with a capacity retain of 73% over 200 cycles. In other works using SDPA as electroactive material in supercapacitor, the retain of 70% in 200 cycles is reported [34]. Also, the reported symmetric supercapacitor PANi/PANi [16] can be used in parallel with a battery only if at least two of them are in the series, due to its low voltage working (~0.8 V). In spite of the high capacitance (~1300 F g^{-1}), it works only at strong acidic medium which is corrosive for the Zn anode, and cannot be used in parallel with Zn secondary battery in a single cell. However, in this work only a single cell of the asymmetric supercapacitor (AC/SDPA) can be easily paralleled with a battery (Zn/SDPA), because the potential working of the supercapacitor AC/SDPA and the battery Zn/SDPA is nearly the same (~1.5 V).

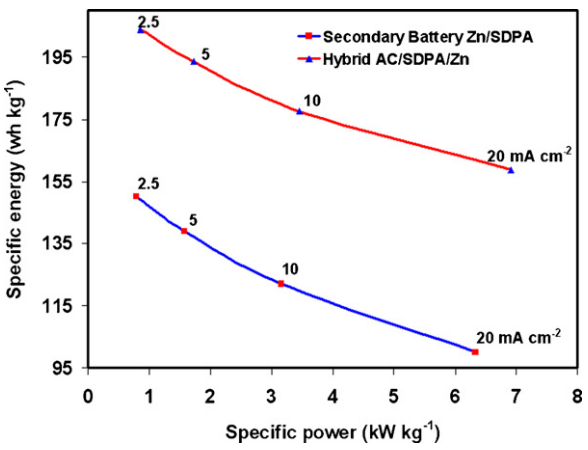

Fig. 6. Relationships between the specific energy and specific power of AC/SDPA/Zn and Zn/SDPA cells at various current densities from 2.5 to 20 mA cm^{-2}.

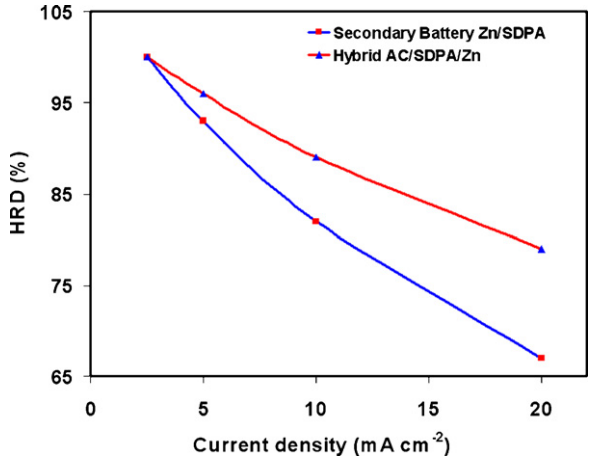

Fig. 7. Relationship between the high rate dischargeability and the current density of the AC/SDPA/Zn and Zn/SDPA cells.

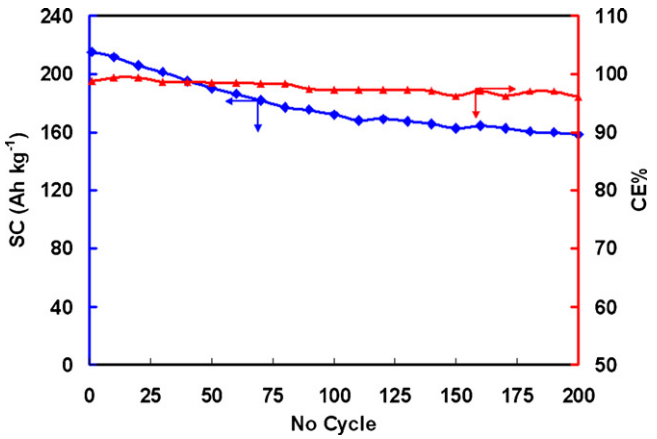

Fig. 8. Dependence of specific capacities and CE% with cycle number for AC/SDPA/Zn hybrid energy storage system. Charge and discharge performed at 2.5 mA cm^{-2} into 1.0 M $ZnCl_2$ and 0.5 M NH_4Cl mixed electrolyte solution.

Other reported works for battery based on the SDPA [21] and the PAN [18] as electroactive materials show the retained capacity of 65% and 60%, respectively, after 200 cycles. So this work with 73% retained capacity shows more than 10% improvement. However, as previously reported [22] electrochemical degradation of the PAN and Zinc passivation can significantly reduce the battery capacity under charge–discharge cycling. It appears that the kinetics of Zn passivation is faster than that of PAN electrochemical degradation.

The coulombic efficiencies (CE %) for the hybrid AC/SDPA/Zn, as calculated according to Eq. (11), are also depicted in Fig. 8.

$$\text{CE } \% = \left(\frac{t_D}{t_c}\right) \times 100 \tag{11}$$

where t_D and t_C are the discharge and charge times, respectively [52]. The results reveal that the hybrid AC/SDPA/Zn shows stable coulombic efficiencies of about 96% over 200 cycles.

4. Conclusions

Using the SDPA at mild pH solutions provides the use of Zn without spontaneous dissolution in addition to retaining the electroactive property of this electrically conducting polymer as compared to the PANi. Nanostructured SDPA was prepared by controlled potential electrochemical oxidation of aniline and *m*-aminobenzoic acid in an aqueous media. This electrically conducting polymer enhanced the performance of energy storage system better than other reported works, which were based on the microstructured SDPA. Using asymmetric configuration of the supercapacitor (AC/SDPA), its operational working voltage was increased up to 1.5 V which is close to the secondary battery Zn/SDPA operational working voltage. So, they can be easily paralleled to achieve a hybrid energy storage system AC/SDPA/Zn. Because the working voltage range and discharging profiles of these two energy storage systems are matched, the hybrid energy storage system shows the advantages of the combination of the secondary battery (high energy) and the supercapacitor (high power) electric delivery. Other advantages of this hybrid energy storage system are its simple construction which does not need a DC–DC converter for supercapacitor voltage adjusting and employing the SDPA as a positive shared electrode. Based on the obtained results, the hybrid system AC/SDPA/Zn reveals good specific energy of 204 Wh kg^{-1} and the specific power of 863 W kg^{-1} at a constant current density of 2.5 mA cm^{-2}.

Acknowledgement

The support of the Tarbiat Modares University Research Council is gratefully acknowledged.

References

[1] R. Valiev, Nature 419 (2002) 887–889.
[2] D.I. Gittins, D. Bethell, D.J. Schiffrin, R.J. Nichols, Nature 408 (2000) 67–69.
[3] C.-j. Liu, U. Burghaus, F. Besenbacher, Z.L. Wang, ACS Nano 4 (2010) 5517–5526.
[4] Y.-G. Guo, J.-S. Hu, L.-J. Wan, Adv. Mater. 20 (2008) 2878–2887.
[5] P.R. Bueno, C. Gabrielli, in: E.R. Leite (Ed.), Nanostructured Materials for Electrochemical Energy Production and Storage, Springer, US, 2009, pp. 81–149.
[6] P. Thounthong, S. Raël, B. Davat, J. Power Sources 193 (2009) 376–385.
[7] X. Zhang, C.C. Mi, A. Masrur, D. Daniszewski, J. Power Sources 185 (2008) 1533–1543.
[8] Y. Zhan, Y. Guo, J. Zhu, H. Wang, J. Power Sources 179 (2008) 745–753.
[9] Z. Jiang, J. Power Sources 177 (2008) 231–238.
[10] N. Yu, L. Gao, S. Zhao, Z. Wang, Electrochim. Acta 54 (2009) 3835–3841.
[11] S.-B. Ma, K.-W. Nam, W.-S. Yoon, X.-Q. Yang, K.-Y. Ahn, K.-H. Oh, K.-B. Kim, Electrochem. Commun. 9 (2007) 2807–2811.
[12] S.H. Choi, J. Kim, Y.S. Yoon, J. Power Sources 138 (2004) 360–363.
[13] B.E. Conway, Electrochemical Supercapacitors: Scientific Fundamentals and Technological Applications, Plenum Press, New York, 1999.
[14] X. Hu, Z. Deng, J. Suo, Z. Pan, J. Power Sources 187 (2009) 635–639.
[15] K.S. Ryu, K.M. Kim, J. Power Sources 165 (2007) 420–426.
[16] K.R. Prasad, N. Munichandraiah, J. Power Sources 112 (2002) 443–451.
[17] L.T. Lam, R. Louey, J. Power Sources 158 (2006) 1140–1148.
[18] K. Ghanbari, M.F. Mousavi, M. Shamsipur, Electrochim. Acta 52 (2006) 1514–1522.
[19] Z. Mandic, M.K. Rokovic, T. Pokupcic, Electrochim. Acta 54 (2009) 2941–2950.
[20] A.A. Syed, M.K. Dinesan, Talanta 38 (1991) 815–837.
[21] M.S. Rahmanifar, M.F. Mousavi, M. Shamsipur, J. Power Sources 110 (2002) 229–232.
[22] M.S. Rahmanifar, M.F. Mousavi, M. Shamsipur, M. Ghaemi, J. Power Sources 132 (2004) 296–301.
[23] M.S. Rahmanifar, M.F. Mousavi, M. Shamsipur, H. Heli, Synth. Met. 155 (2005) 480–484.
[24] M.S. Rahmanifar, M.F. Mousavi, M. Shamsipur, S. Riahi, Polym. Degrad. Stab. 91 (2006) 3463–3468.
[25] E. Salamifar, M.A. Mehrgardi, M.F. Mousavi, Electrochim. Acta 54 (2009) 4638–4646.
[26] E.Y. Kim, M.H. Lee, B.S. Moon, C.J. Lee, S.B. Rhee, J. Electrochem. Soc. 141 (1994) L26–L28.
[27] A. Malinauskas, J. Power Sources 126 (2004) 214–220.
[28] H. Varela, S.L. de Albuquerque Maranhão, R.M.Q. Mello, E.A. Ticianelli, R.M. Torresi, Synth. Met. 122 (2001) 321–327.
[29] H. Varela, R.M. Torresi, J. Electrochem. Soc. 147 (2000) 665–670.
[30] C. Barbero, M.C. Miras, B. Schnyder, O. Haas, R. Kotz, J. Mater. Chem. 4 (1994) 1775–1783.
[31] H. Varela, R.M. Torresi, D.A. Buttry, J. Electrochem. Soc. 147 (2000) 4217–4223.
[32] C. Barbero, R. Kotz, Adv. Mater. 6 (1994) 577–580.
[33] H. Varela, R.M. Torresi, D.A. Buttry, J. Braz. Chem. Soc. 11 (2000) 32–38.
[34] H.R. Ghenaatian, M.F. Mousavi, S.H. Kazemi, M. Shamsipur, Synth. Met. 159 (2009) 1717–1722.
[35] J.H. Park, O.O. Park, J. Power Sources 111 (2002) 185–190.
[36] X.F. Wang, D.B. Ruan, D.Z. Wang, J. Liang, Acta Phys. Chim. Sin. 21 (2005) 261–266.
[37] S. Ghasemi, M.F. Mousavi, H. Karami, M. Shamsipur, S.H. Kazemi, Electrochim. Acta 52 (2006) 1596–1602.
[38] H. Karami, M. Shamsipur, S. Ghasemi, M.F. Mousavi, J. Power Sources 164 (2007) 896–904.
[39] H. Karami, M.F. Mousavi, M. Shamsipur, J. Power Sources 117 (2003) 255–259.
[40] H. Karami, M.F. Mousavi, M. Shamsipur, J. Power Sources 124 (2003) 303–308.
[41] H. Karami, M.F. Mousavi, M. Shamsipur, S. Riahi, J. Power Sources 154 (2006) 298–307.
[42] K. Ghanbari, M.F. Mousavi, M. Shamsipur, H. Karami, J. Power Sources 170 (2007) 513–519.
[43] V. Gupta, N. Miura, Electrochem. Commun. 7 (2005) 995–999.
[44] N.T. Kemp, J.W. Cochrane, R. Newbury, Synth. Met. 159 (2009) 435–444.
[45] B.C. Bunker, P.C. Rieke, B.J. Tarasevich, A.A. Campbell, G.E. Fryxell, G.L. Graff, L. Song, J. Liu, J.W. Virden, G.L. McVay, Science 264 (1994) 48–55.
[46] H. Zhang, J. Wang, Z. Wang, F. Zhang, S. Wang, Synth. Met. 159 (2009) 277–281.
[47] C. Liu, K. Hayashi, K. Toko, Electrochem. Commun. 12 (2010) 36–39.
[48] X. Liu, P.G. Pickup, J. Power Sources 176 (2008) 410–416.
[49] X.J. He, Y.J. Geng, S. Oke, K. Higashi, M. Yamamoto, H. Takikawa, Synth. Met. 159 (2009) 7–12.
[50] T. Cottineau, M. Toupin, T. Delahaye, T. Brousse, D. Bélanger, Appl. Phys. A: Mater. 82 (2006) 599–606.
[51] H. Mi, X. Zhang, S. Yang, X. Ye, J. Luo, Mater. Chem. Phys. 112 (2008) 127–131.
[52] W.-C. Chen, T.-C. Wen, J. Power Sources 117 (2003) 273–282.